Journal of Physics: Conference Series **633** (2015) 012094 doi:10.1088/1742-6596/633/1/012094

Modeling of the Calcium/Phosphorus Mass ratio for Breast Imaging

N Martini[1], V Koukou[1], C Michail[2], P Sotiropoulou[1], N Kalyvas[2], I Kandarakis[2], G Nikiforidis[1] and G Fountos[2]

[1] Department of Medical Physics, Medical School, University of Patras, 265 00 Patras, Greece
[2] Radiation Physics, Materials Technology and Biomedical Imaging Laboratory, Department of Biomedical Engineering, Technological Educational Institute of Athens, Egaleo, 122 10 Athens, Greece

E-mail: gfoun@teiath.gr

Abstract. Breast microcalcifications are mainly composed of calcite ($CaCO_3$), calcium oxalate (CaC_2O_4) and apatite (a calcium-phosphate mineral form). Any pathologic alteration (carcinogenesis) of the breast may produce apatite. In the present simulation study, an analytical model was implemented in order to distinguish malignant and non-malignant lesions. The Calcium/Phosphorus (Ca/P) mass ratio and the standard deviation (SD) of the calcifications were calculated. The size of the calcifications ranged from 100 to 1000 μm, in 50 μm increments. The simulation was performed for hydroxyapatite, calcite and calcium oxalate calcifications. The optimum pair of energies for all calcifications was 22keV and 50keV. Hydroxyapatite and calcite calcifications were sufficiently characterized through their distinct confidence interval (99.7%, 3SD) values for calcifications sizes above 500 μm, while the corresponding sizes for hydroxyapatite and calcium oxalate characterization were found above 250 μm. Initial computer simulation results indicate that the proposed method can be used in breast cancer diagnosis, reducing the need for invasive methods, such as biopsies.

1. Introduction

The most common cause of cancer deaths is the breast cancer, responsible for approximately 16% of cancer deaths in adult women [1]. Calcifications are a diagnostic key for the localization of malignancy. Type I calcifications are composed of calcium oxalate (CaC_2O_4), and are associated with benign lesions of the breast [2,3]. Type II calcifications are composed of calcium phosphate, mainly hydroxyapatite (HAp), and calcium carbonate ($CaCO_3$) associated with malignant and benign breast conditions, respectively [4,5]. Where suspected calcifications are detected, traditionally a needle biopsy follows in order to determine whether the associated lesion is malignant or benign [6]. This could be avoided if a rapid and safe noninvasive method was available [7].

In this simulation study, a dual energy method was used for the calculation of the Ca/P mass ratio and the standard deviation (SD) of the calcifications. The study was performed for hydroxyapatite calcifications, indicating malignancy, as well as for calcite and calcium oxalate calcifications, indicating benign lesions. The optimum pair of energies for all calcifications was 22keV and 50keV. Hydroxyapatite and calcite calcifications thicker than 500 μm were sufficiently characterized through their distinct confidence interval (99.7%, 3SD) values, while the corresponding sizes for hydroxyapatite and calcium oxalate characterization were found above 250 μm. Initial simulation results indicate that the proposed method can be used in breast cancer diagnosis, reducing the need for invasive methods, such as biopsies.

2. Materials and Methods

An analytical model was developed in order to determine the calcifications' Ca/P mass ratio and the Coefficient of Variation (CV), assuming only Poisson distribution. The breast is considered to be composed of a mixture of 50% adipose and 50% glandular tissue, of a thickness t_m and a calcification with thickness t_c. Malignant calcifications were simulated with hydroxyapatite ($Ca_{10}(PO_4)_6(OH)_2$) having a density of 3.18g/cm^3 [8]. For the simulation of benign calcifications calcium carbonate ($CaCO_3$) and calcium oxalate (CaC_2O_4) with densities of 2.93g/cm^3 and 2.20g/cm^3 [9], respectively, were used.

A 4cm compressed breast [10] was irradiated twice. In the first irradiation, for the low- and high-energy, the intensities attenuate after passing through the mixture only, while in the second irradiation the intensities attenuate after passing through the mixture and calcification. The examined calcification thicknesses were 100 μm to 1000 μm (microcalcifications), and 550 to 1000 μm (macrocalcifications) in 50 μm increments respectively.

In order to determine the Ca/P mass ratio, the above attenuated intensities were calculated according to equations (1) & (2) considering monoenergetic X-rays ranging from 15 to 70keV, in 1keV increments. The attenuated intensities, for the low- and high-energy, after passing through a mixture of 50% adipose and 50% glandular tissue can be expressed as:

$$I_{m,E_i} = I_{o,E_i} \cdot e^{-\left(\frac{\mu}{\rho_{a(E_i)}} \cdot \rho_a + \frac{\mu}{\rho_{g(E_i)}} \cdot \rho_g\right) \cdot 0.5 \cdot T}, \quad i = l, h \tag{1}$$

where, I_{o,E_l} and I_{o,E_h} are the unattenuated low- and high-energy photon intensity, per unit energy $\left(photons/cm^2 keV\right)$, at the detector input. The energy-dependent mass attenuation coefficients $\left(cm^2/g\right)$, as well as the density $\left(g/cm^3\right)$ for adipose and glandular are given by $\mu/\rho_{a(E_t)}$, $\mu/\rho_{g(E_t)}$, respectively.

The corresponding attenuated intensities by both the mixture and the calcification were calculated as follows:

$$I_{c,E_i} = I_{o,E_i} \cdot e^{-\frac{\mu}{\rho_{Ca(E_i)}} \cdot \rho_{Ca} \cdot t_{Ca} - \frac{\mu}{\rho_{j(E_i)}} \cdot \rho_j \cdot t_j - \left(\frac{\mu}{\rho_{a(E_i)}} \cdot \rho_a + \frac{\mu}{\rho_{g(E_i)}} \cdot \rho_g\right) \cdot 0.5 \cdot t_m}, \quad i = l, h,\ j = PO_4, CO_3, C_2O_4 \tag{2}$$

where, the energy-dependent mass attenuation coefficients $\left(cm^2/g\right)$, as well as the density $\left(g/cm^3\right)$ for adipose, glandular, calcium, phosphate, carbonate and oxalate are given by $\mu/\rho_{a(E_t)}$, $\mu/\rho_{g(E_t)}$, $\mu/\rho_{Ca(E_t)}$, $\mu/\rho_{PO_4(E_t)}$, $\mu/\rho_{CO_3(E_t)}$, $\mu/\rho_{C_2O_4(E_t)}$ and $\rho_a, \rho_g, \rho_{Ca}, \rho_{PO_4}, \rho_{CO_3}, \rho_{C_2O_4}$, respectively.

Data for the elemental compositions of glandular and adipose tissues in a human breast were used for the mass attenuation coefficients determination [11]. The densities used were 0.93 g/cm^3 for

adipose tissue and 1.04 g/cm^3 for glandular tissue [11]. Mass attenuation coefficients of the materials used in this work were computed by XMuDat software from NIST [12].

Thus, the Ca/P mass ratio can be determined by [13,14]:

$$\frac{Ca}{P}=\frac{\ln\frac{I_{m,E_l}}{I_{c,E_l}}\cdot\left(\frac{\mu}{\rho_{PO_4,E_h}}\cdot\rho_{HAp}-\left(\frac{\mu}{\rho_{a,E_h}}\cdot\rho_a+\frac{\mu}{\rho_{g,E_h}}\cdot\rho_g\right)\cdot 0.5\right)-\ln\frac{I_{m,E_h}}{I_{c,E_h}}\cdot\left(\frac{\mu}{\rho_{PO_4,E_l}}\cdot\rho_{HAp}-\left(\frac{\mu}{\rho_{a,E_l}}\cdot\rho_a+\frac{\mu}{\rho_{g,E_l}}\cdot\rho_g\right)\cdot 0.5\right)}{-\ln\frac{I_{m,E_l}}{I_{c,E_l}}\cdot\left(\frac{\mu}{\rho_{Ca,E_h}}\cdot\rho_{HAp}-\left(\frac{\mu}{\rho_{a,E_h}}\cdot\rho_a+\frac{\mu}{\rho_{g,E_h}}\cdot\rho_g\right)\cdot 0.5\right)+\ln\frac{I_{m,E_h}}{I_{c,E_h}}\cdot\left(\frac{\mu}{\rho_{Ca,E_l}}\cdot\rho_{HAp}-\left(\frac{\mu}{\rho_{a,E_l}}\cdot\rho_a+\frac{\mu}{\rho_{g,E_l}}\cdot\rho_g\right)\cdot 0.5\right)}\cdot 3.0679 \quad (3)$$

The simulation was performed for hydroxyapatite, calcite and calcium oxalate indicating malignant (hydroxyapatite) and benign (calcite and calcium oxalate) calcifications. When malignant calcifications are present, the model estimates the Ca/P mass ratio of hydroxyapatite where Ca and P are both elements in this molecule. On the contrary, P is not present in benign calcifications. In this case, the model calculates an effective-Ca/P mass ratio, which differs compared to that calculated for hydroxyapatite. The differences between these Ca/P mass ratios were determined.

3. Results and Discussion

For all the calcification sizes examined, the optimum pair of energies was 22keV and 50keV for the low- and high-energy, respectively.

Figure 1 shows the Ca/P mass ratios of hydroxyapatite and calcite for both microcalcifications and macrocalcifications. In all figures error bars correspond to 3SD. Calcifications thicker than 500 μm can be discriminated, since the confidence interval (99.7%, 3SD) for the estimated Ca/P mass ratios, between calcite and hydroxyapatite, can be clearly distinguished. This allows characterization between malignant and benign calcifications. The corresponding Ca/P mass ratios and SDs were 1.2782 and 0.0862 for calcite, while for hydroxyapatite were 1.9713 and 0.1366, respectively.

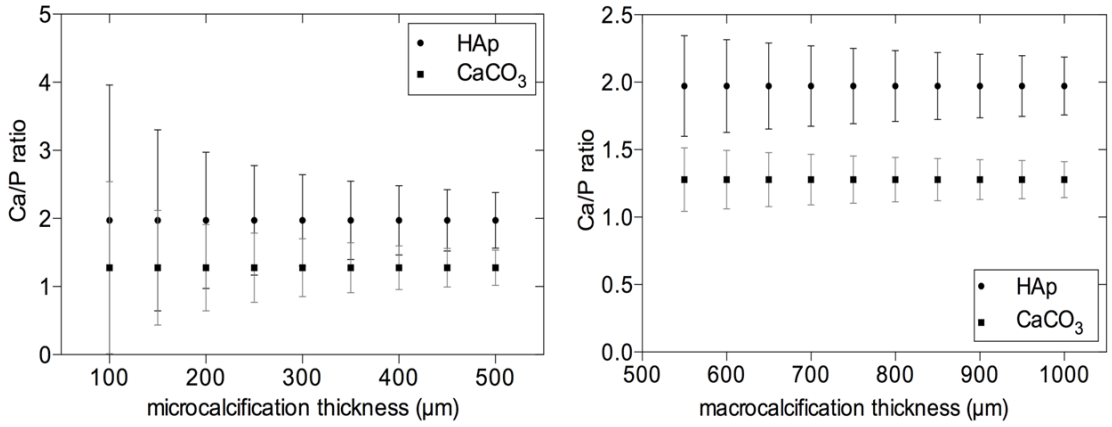

Figure 1. Ca/P_{HAp} and Ca/P_{CaCO3} as a function of microcalcifications (left) and macrocalcifications (right) sizes.

Figure 2 shows the Ca/P mass ratios of hydroxyapatite and calcium oxalate for both microcalcifications and macrocalcifications. Discrimination between malignant (hydroxyapatite) and benign (calcium oxalate) microcalcifications, with sizes above 250 μm, can be observed. The corresponding Ca/P mass ratios and SDs were 0.7198 and 0.1484 for calcium oxalate, and for hydroxyapatite were 1.9713 and 0.2679, respectively.

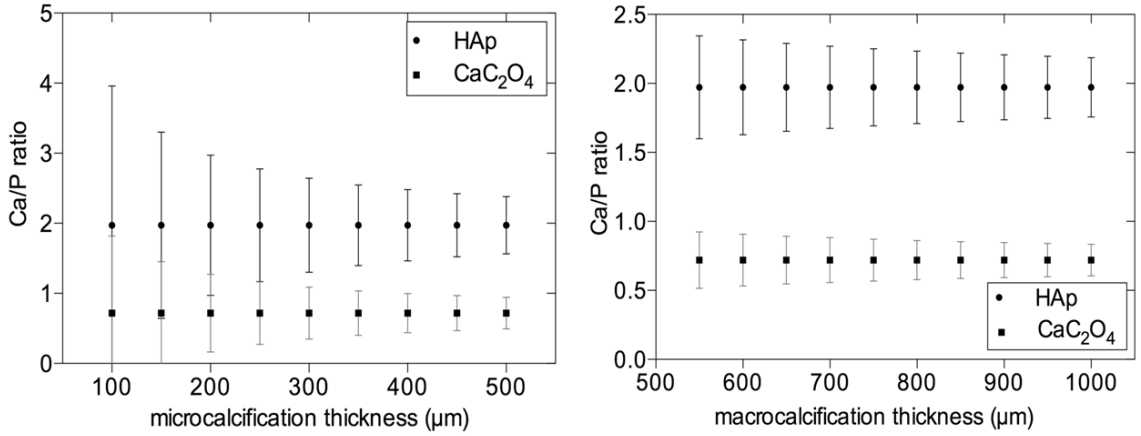

Figure 2. Ca/P_{HAp} and Ca/P_{CaCO3} as a function of microcalcifications (left) and macrocalcifications (right) sizes.

4. Conclusion

In this study characterization of breast calcifications through the determination of the Calcium/Phosphorus (Ca/P) mass ratio was performed, by implementing a dual energy method through analytical modeling. Sufficient characterization resulted between malignant and non-malignant calcifications for sizes above 500 μm. The corresponding size between hydroxyapatite and calcite or calcium oxalate was 250 μm, respectively. The method implemented in this work could be used to discriminate between malignant and benign lesions, reducing the need for biopsies.

Acknowledgement

This research has been co-funded by the European Union (European Social Fund) and Greek national resources under the framework of the "Archimedes III: Funding of Research Groups in TEI of Athens" project of the "Education & Lifelong Learning" Operational Programme.

5. References

[1] World Health Organization 2008 World health statistics 2008
[2] Frappart L, Remy I, Lin HC, Bremond A, Raudrant D, Grousson B, and Vauzelle JL 1986 *Virchows Arch A* **410** 179
[3] Busing CM, Keppler U, and Menges V 1981 *Virchows Arch [Pathol Anat]* **393** 307
[4] Haka AS, Shafer-Peltier KE, Fitzmaurice M, Crowe J, Dasari RR, and Feld MS 2002 *Cancer Res.* **62** 5375
[5] Koukou V, Martini N, Fountos G, Sotiropoulou P, Michail C, Valais I, Kandarakis I and Nikiforidis G 2014 *IFMBE Proceedings* **41** 459
[6] Arkidis N, Skiadopoulos S, Sakellaropoulos F, Karahaliou A, Vassiou K, Kazantzi A, and ostaridou L 2014 *Phys Medica* **30** e75
[7] Matousek P and Stone N 2013 *J Biophoton* **6** 7
[8] Gong JK, Arnold JS, and Cohn SH 1964 *Anat. Rec.* **149** 319
[9] Brandan M and Ramirez V 2006 *Phys. Med. Biol.* **51** 2307
[10] Samei E and Saunders RSJr 2011 *Phys. Med. Biol.* **56** 6359
[11] Hammerstein R, Miller D, White D, Masterson M, Woodward H and Laughlin J 1979 *Radiology* **130** 485

[12] Hubbell J and Seltzer S 1995 US Department of commerce NISTIR 5632
[13] Fountos G, Yahumura S, and Glaros D 1997 *Med. Phys.* **24** 1303
[14] Sotiropoulou P, Fountos G, Martini N, Koukou V, C Michail C, Valais I, Kandarakis I and Nikiforidis G 2015 *Phys Medica* doi:10.1016/j.ejmp.2015.01.019